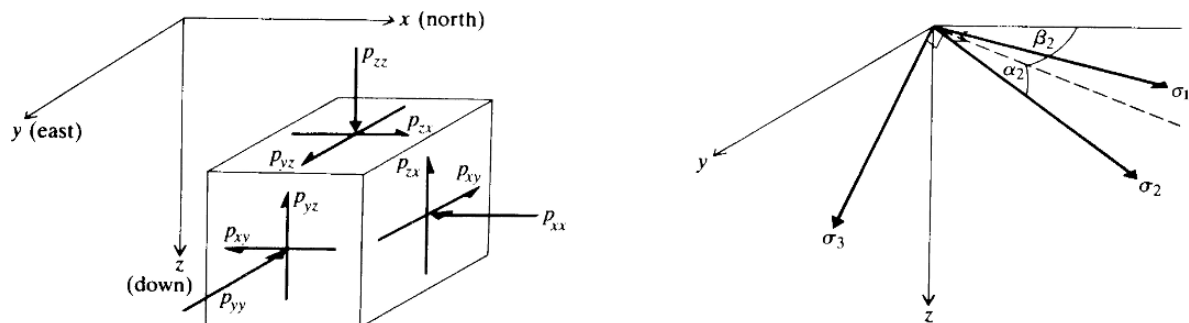# 5 Pre-mining state of stress

5.1 Specification of the pre-mining state of stress

The design of an underground structure in rock differs from other types of structural design in the nature of the loads operating in the system. In conventional surface structures, the geometry of the structure and its operating duty define the loads imposed on the system. For an underground rock structure, the rock medium is subject to initial stress prior to excavation. The final, post-excavation state of stress in the structure is the resultant of the initial state of stress and stresses induced by excavation. Since induced stresses are directly related to the initial stresses, it is clear that specification and determination of the pre-mining state of stress is a necessary precursor to any design analysis.

The method of specifying the *in situ* state of stress at a point in a rock mass, relative to a set of reference axes, is demonstrated in Figure 5.1. A convenient set of Cartesian global reference axes is established by orienting the x axis towards mine north, y towards mine east, and z vertically downwards. The ambient stress components expressed relative to these axes are denoted p_{xx}, p_{yy}, p_{zz}, p_{xy}, p_{yz}, p_{zx}. Using the methods established in Chapter 2, it is possible to determine, from these components, the magnitudes of the field principal stresses $p_i (i = 1, 2, 3)$, and the respective vectors of direction cosines $(\lambda_{xi}, \lambda_{yi}, \lambda_{zi})$ for the three principal axes. The corresponding direction angles yield a dip angle, α_i, and a bearing, or dip azimuth, β_i, for each principal axis. The specification of the pre-mining state of stress is completed by defining the ratio of the principal stresses in the form $p_1 : p_2 : p_3 = 1.0 : q : r$ where both q and r are less than unity.

The assumption made in this discussion is that it is possible to determine the *in situ* state of stress in a way which yields representative magnitudes of the components of the field stress tensor throughout a problem domain. The state of stress in the rock mass is inferred to be spatially quite variable, due to the presence of structural features such as faults or local variation in rock material properties. Spatial variation in the field stress tensor may be sometimes observed as an apparent violation of the equation of equilibrium for the global z (vertical) direction. Since the ground surface is always traction-free, simple statics requires that the vertical normal stress component at a

Figure 5.1 Method of specifying the *in situ* state of stress relative to a set of global reference axes.

142

sub-surface point be given by

$$p_{zz} = \gamma z \tag{5.1}$$

where γ is the rock unit weight, and z is the depth below ground surface.

Failure to satisfy this equilibrium condition (equation 5.1) in any field determination of the pre-mining state of stress may be a valid indication of heterogeneity of the stress field. For example, the vertical normal stress component might be expected to be less than the value calculated from equation 5.1, for observations made in the axial plane of an anticlinal fold.

A common but unjustified assumption in the estimation of the *in situ* state of stress is a condition of uniaxial strain ('complete lateral restraint') during development of gravitational loading of a formation by superincumbent rock. For elastic rock mass behaviour, horizontal normal stress components are then given by

$$p_{xx} = p_{yy} = \left(\frac{\nu}{1-\nu}\right) p_{zz} \tag{5.2}$$

where ν is Poisson's ratio for the rock mass.

If it is also assumed that the shear stress components p_{xy}, p_{yz}, p_{zx} are zero, the normal stresses defined by equations 5.1 and 5.2 are principal stresses.

Reports and summaries of field observations (Hooker *et al.*, 1972; Brown and Hoek, 1978) indicate that for depths of stress determinations of mining engineering interest, equation 5.2 is rarely satisfied, and the vertical direction is rarely a principal stress direction. These conditions arise from the complex load path and geological history to which an element of rock is typically subjected in reaching its current equilibrium state during and following orebody formation.

5.2 Factors influencing the *in situ* state of stress

The ambient state of stress in an element of rock in the ground subsurface is determined by both the current loading conditions in the rock mass, and the stress path defined by its geologic history. Stress path in this case is a more complex notion than that involved merely in changes in surface and body forces in a medium. Changes in the state of stress in a rock mass may be related to temperature changes and thermal stress, and chemical and physicochemical processes such as leaching, precipitation and recrystallisation of constituent minerals. Mechanical processes such as fracture generation, slip on fracture surfaces and viscoplastic flow throughout the medium, can be expected to produce both complex and heterogeneous states of stress. Consequently, it is possible to describe, in only semi-quantitative terms, the ways in which the current observed state of a rock mass, or inferred processes in its geologic evolution, may determine the current ambient state of stress in the medium. The following discussion is intended to illustrate the role of common and readily comprehensible factors on pre-mining stresses.

5.2.1 Surface topography

Previous discussion has indicated that, for a flat ground surface, the average vertical stress component should approach the depth stress (i.e. $p_{zz} = \gamma z$). For irregular

143
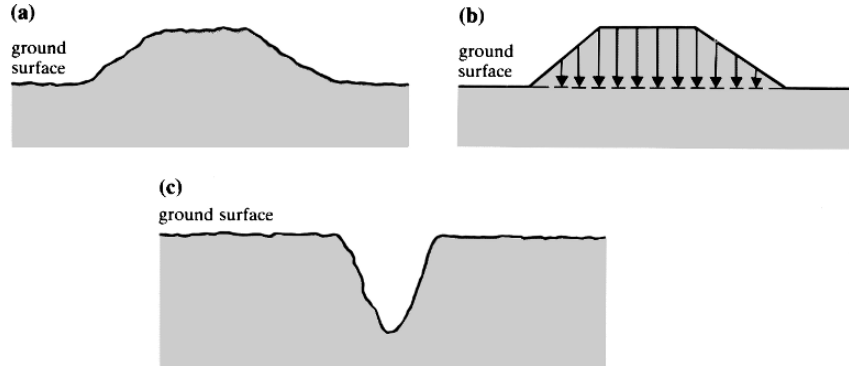
Figure 5.2 The effect of irregular surface topography (a) on the subsurface state of stress may be estimated from a linearised surface profile (b). A V-notch valley (c) represents a limiting case of surface linearisation.

surface topography, such as that shown in Figure 5.2a, the state of stress at any point might be considered as the resultant of the depth stress and stress components associated with the irregular distribution of surface surcharge load. An estimate of the latter effect can be obtained by linearising the surface profile, as indicated in Figure 5.2b. Expressions for uniform and linearly varying strip loads on an elastic half-space can be readily obtained by integration of the solution for a line load on a half-space (Boussinesq, 1883). From these expressions, it is possible to evaluate the state of stress in such locations as the vicinity of the subsurface of the base of a V-notch valley (Figure 5.2c). Such a surface configuration would be expected to produce a high horizontal stress component, relative to the vertical component at this location. In all cases, it is to be expected that the effect of irregular surface topography on the state of stress at a point will decrease rapidly as the distance of the point below ground surface increases. These general notions appear to be confirmed by field observations (Endersbee and Hofto, 1963).

5.2.2 Erosion and isostasy

Erosion of a ground surface, either hydraulically or by glaciation, reduces the depth of rock cover for any point in the ground subsurface. It can be reasonably assumed that the rock mass is in a lithologically stable state prior to erosion, and thus that isostasy occurs under conditions of uniaxial strain in the vertical direction. Suppose after deposition of a rock formation, the state of stress at a point P below the ground surface is given by

$$p_x = p_y = p_z = p$$

If a depth h_e of rock is then removed by erosion under conditions of uniaxial strain, the changes in the stress components are given by

$$\Delta p_z = -h_e\gamma, \quad \Delta p_x = \Delta p_y = v/(1-v)\Delta p_z = -v/(1-v)h_e\gamma$$

and the post-erosion values of the stress components are

$$p_{xf} = p_{yf} = p - v/(1-v)h_e\gamma, \quad p_{zf} = p - h_e\gamma$$

Because $v < 0.5$, from this expression it is clear that, after the episode of erosion, the

144

horizontal stresses are reduced by amounts less than the reduction in vertical stress; i.e.

$$p_{xf}, p_{yf} > p_{zf}$$

or the ratios of the stresses p_{xf}/p_{zf}, p_{yf}/p_{zf} are greater than unity. For a point at shallow current depth h_c, it can be shown that, for $h_e \gg h_c$, is possible for the ratios of the horizontal stresses to the vertical stress to achieve very high values indeed.

From this analysis, it can also be deduced that the horizontal/vertical stress ratio decreases as the current depth h_c increases, approaching the pre-erosion value when h_c is significantly greater than h_e.

5.2.3 Residual stress

Residual stresses exist in a finite body when its interior is subject to a state of stress in the absence of applied surface tractions. The phenomenon has long been recognised in the mechanics of materials. For example, Love (1944) describes the generation of residual stresses in a cast-iron body on cooling, due to the exterior cooling more rapidly than the interior. Timoshenko and Goodier (1970) also discuss the development of residual (or initial) stresses in common engineering materials. In general, residual stresses may be related to physical or chemical processes occurring non-homogeneously in restricted volumes of material. For example, non-uniform cooling of a rock mass, or the presence in a rock mass subject to uniform cooling, of contiguous lithological units with different coefficients of thermal expansion, will produce states of stress which are locally 'locked-in'.

Processes other than cooling that produce residual stresses may involve local mineralogical changes in the rock medium. Local recrystallisation in a rock mass may be accompanied by volumetric strain. Changes in the water content of a mineral aggregation, by absorption or exudation and elimination of chemically or physically associated water, can result in strains and residual stresses similar in principle to those associated with spatially non-uniform cooling.

A comprehensive understanding of the thermal history and subtle geologic evolution of the members of a rock formation is not considered a practical possibility. The problem of residual stresses therefore remains an inhibiting factor in predicting the ambient state of stress in a rock mass, from either basic mechanics or detailed geological investigations. The inverse process may be a more tractable proposition; i.e. anomalous or non-homogeneous states of stress in a formation may be related to the features or properties of the rock mass which reflect the spatial non-uniformity of its thermal, chemical or petrological history.

5.2.4 Inclusions

Inclusions in a rock mass are lithological units that post-date the formation of the host rock mass. Common inclusions are extrusive features such as dykes and sills, and veins of such minerals as quartz and fluorspar. The existence of a vertical, subplanar inclusion in a rock mass may have influenced the current *in situ* state of stress in two ways. First, if the inclusion were emplaced under pressure against the horizontal passive resistance of the surrounding rock, a high-stress component would operate perpendicular to the plane of inclusion. A second possible influence of an inclusion is related to the relative values of the deformation moduli of the inclusion and the

145

surrounding rock. Any loading of the system, for example by change of effective stress in the host rock mass or imposed displacements in the medium by tectonic activity, will generate relatively high or low stresses in the inclusion, compared with those in the host rock mass. A relatively stiff inclusion will be subject to relatively high states of stress, and conversely. An associated consequence of the difference in elastic moduli of host rock and inclusion is the existence of high-stress gradients in the host rock in the vicinity of the inclusion. In contrast, the inclusion itself will be subject to a relatively homogeneous state of stress (Savin, 1961).

An example of the effect of an inclusion on the ambient state of stress is provided by studies of conditions in and adjacent to dykes in the Witwatersrand Quartzite. The high elastic modulus of dolerite, compared with that of the host quartzite, should lead to a relatively high state of stress in the dyke, and a locally high stress gradient in the dyke margins. These effects appear to be confirmed in practice (Gay, 1975).

5.2.5   Tectonic stress

The state of stress in a rock mass may be derived from a pervasive force field imposed by tectonic activity. Stresses associated with this form of loading operate on a regional scale, and may be correlated with such structural features as thrust faulting and folding in the domain. Active tectonism need not imply that an area be seismically active, since elements of the rock mass may respond viscoplastically to the imposed state of stress. However, the stronger units of a tectonically stressed mass should be characterised by the occurrence of one subhorizontal stress component significantly greater than both the overburden stress and the other horizontal component. It is probable also that this effect should persist at depth. The latter factor may therefore allow distinction between near-surface effects, related to erosion, and latent tectonic activity in the medium.

5.2.6   Fracture sets and discontinuities

The existence of fractures in a rock mass, either as sets of joints of limited continuity, or as major, persistent features transgressing the formation, constrains the equilibrium state of stress in the medium. Thus vertical fractures in an uplifted or elevated rock mass, such as a ridge, can be taken to be associated with low horizontal stress components. Sets of fractures whose orientations, conformation and surface features are compatible with compressive failure in the rock mass, can be related to the properties of the stress field inducing fracture development (Price, 1966). In particular, a set of conjugate faults is taken to indicate that the direction of the major principal field stress prior to faulting coincides with the acute bisector of the faults' dihedral angle, the minor principal stress axis with the obtuse bisector, and the intermediate principal stress axis with the line of intersection of the faults (Figure 5.3). This assertion is based on a simple analogy with the behaviour of a rock specimen in true triaxial compression. Such an interpretation of the orientation of the field principal stresses does not apply to the state of stress prevailing following the episode of fracture. In fact, the process of rock mass fracture is intrinsically an energy dissipative and stress redistributive event.

The implication of the stress redistribution during any clastic episode is that the ambient state of stress may be determined by the need to maintain equilibrium conditions on the fracture surfaces. It may bear little relation to the pre-fracture state of stress. A further conclusion, from considerations of the properties of fractured rock,

146
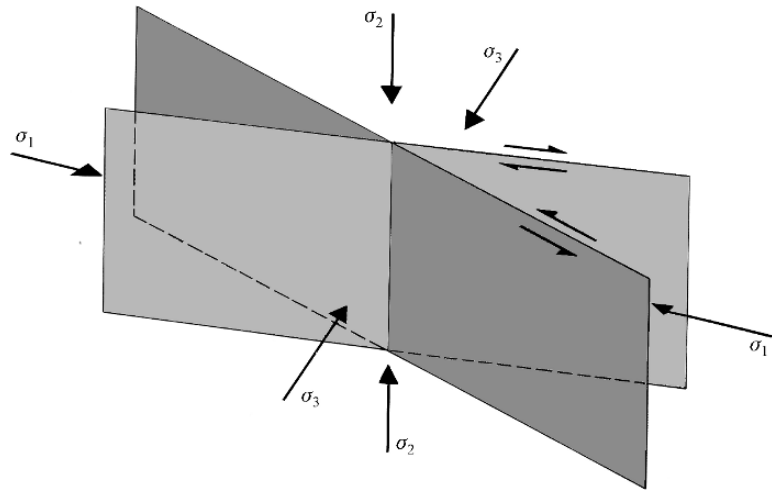
Figure 5.3 Relation between fault geometry and the field stresses causing faulting.

and of significance in site investigation, relates to the problem of spatial variability of the field stress tensor. A fracture field in a rock mass is usually composed of members which are variably oriented. It is inferred that a mechanically compatible stress field may also be locally variable, in both magnitudes and orientations of the principal stresses. A heterogeneous stress field is thus a natural consequence of an episode of faulting, shearing or extensive slip, such as occurs between beds in parallel folding. Successive episodes of fracturing, where, for example, one fault set transgresses an earlier set, may be postulated to lead to increasing complexity in the stress distribution throughout the medium.

It is clear from this brief discussion that the ambient, subsurface state of stress in a rock mass presents prohibitive difficulty in estimation *ab initio*. Its direct determination experimentally also presents some difficulty. In particular, the spatial variability of the stress tensor suggests that any single experimental determination may bear little relation to volume averages of the tensor components. In the design of a mine excavation or mine structure, it is the average state of stress in the zone of influence of the structure which exerts a primary control on the post-excavation stress distribution in the excavation near-field rock. The requirements for successful definition of the *in situ* state of stress are a technique for a local determination of the stress tensor, and a strategy for integration of a set of observations to derive a representative solution for the field stress tensor throughout the sampled volume.

5.3 Methods of *in situ* stress determination

5.3.1 General procedures

The need for reliable estimates of the pre-mining state of stress has resulted in the expenditure of considerable effort in the development of stress measurement devices and procedures. Methods developed to date exploit several separate and distinct principles in the measurement methodology, although most methods use a borehole to gain access to the measurement site. The most common set of procedures is based on determination of strains in the wall of a borehole, or other deformations of the borehole,

147

induced by overcoring that part of the hole containing the measurement device. If sufficient strain or deformation measurements are made during this stress-relief operation, the six components of the field stress tensor can be obtained directly from the experimental observations using solution procedures developed from elastic theory. The second type of procedure, represented by flatjack measurements and hydraulic fracturing (Haimson, 1978), determines a circumferential normal stress component at particular locations in the wall of a borehole. At each location, the normal stress component is obtained by the pressure, exerted in a slot or fissure, which is in balance with the local normal stress component acting perpendicular to the measurement slot. The circumferential stress at each measurement location may be related directly to the state of stress at the measurement site, preceding boring of the access hole. If sufficient boundary stress determinations are made in the hole periphery, the local value of the field stress tensor can be determined directly.

The third method of stress determination is based on the analysis and interpretation of patterns of fracture and rupture around deep boreholes such as oil and gas wells. Although such 'borehole breakouts' are a source of difficulty in petroleum engineering, they are invaluable for estimating the state of stress in the lithosphere.

For characterising the state of stress on a regional scale, a method which is fundamentally different from the three described above was formulated by Mukhamediev (1991). It relies on the analysis in the domain of interest of stress trajectories, derived from other types of stress measurement, to reconstruct the distribution of principal stresses throughout the block. The method is discussed later in relation to the world stress map.

The importance of the *in situ* state of stress in rock engineering has been recognized by the documentation of ISRM Suggested Methods of rock stress estimation, reported by Hudson *et al.* (2003), Sjöberg *et al.* (2003) and Haimson and Cornet (2003).

5.3.2 Triaxial strain cell

The range of devices for direct and indirect determination of *in situ* stresses includes photoelastic gauges, USBM borehole deformation gauges, and biaxial and triaxial strain cells. The soft inclusion cell, as described by Leeman and Hayes (1966) and Worotnicki and Walton (1976) is the most convenient of these devices, since it allows determination of all components of the field stress tensor in a single stress relief operation. Such a strain cell, as shown in Figure 5.4a, consists of at least three strain rosettes, mounted on a deformable base or shell. The method of operation is indicated in Figures 5.4b, c and d. The cell is bonded to the borehole wall using a suitable epoxy or polyester resin. Stress relief in the vicinity of the strain cell induces strains in the gauges of the strain rosettes, equal in magnitude but opposite in sign to those originally existing in the borehole wall. It is therefore a simple matter to establish, from measured strains in the rosettes, the state of strain in the wall of the borehole prior to stress relief. These borehole strain observations are used to deduce the local state of stress in the rock, prior to drilling the borehole, from the elastic properties of the rock and the expressions for stress concentration around a circular hole.

The method of determination of components of the field stress tensor from borehole strain observations is derived from the solution (Leeman and Hayes, 1966) for the stress distribution around a circular hole in a body subject to a general triaxial state of stress. Figure 5.5a shows the orientation of a stress measurement hole, defined

148

(a)
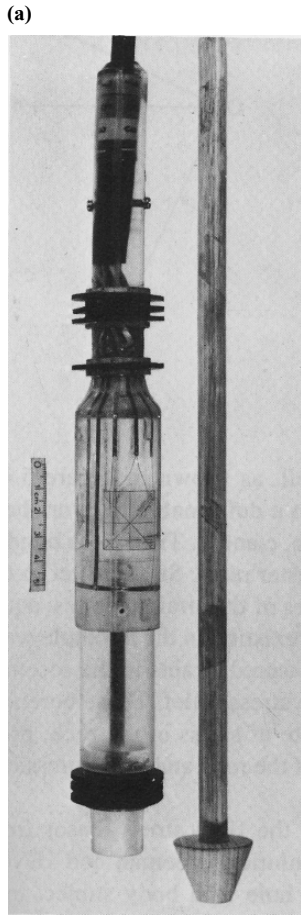
by dip, α, and dip direction, β, relative to a set of global axes x, y, z. Relative to these axes, the ambient field stress components (prior to drilling the hole) are p_{xx}, p_{yy}, P_{zz}, p_{xy}, p_{yz}, p_{zx}. A convenient set of local axes, l, m, n, for the borehole is also shown in Figure 5.5a, with the n axis directed parallel to the hole axis, and the m axis lying in the horizontal (x, y) plane. The field stress components expressed relative to the hole local axes, i.e. p_{ll}, p_{ln}, etc., are readily related to the global components p_{xx}, p_{xz}, etc., through the stress transformation equation and a rotation matrix defined by

$$[\mathbf{R}] = \begin{bmatrix} \lambda_{xl} & \lambda_{xm} & \lambda_{xn} \\ \lambda_{yl} & \lambda_{ym} & \lambda_{yn} \\ \lambda_{zl} & \lambda_{zm} & \lambda_{zn} \end{bmatrix} = \begin{bmatrix} -\sin\alpha\cos\beta & \sin\beta & \cos\alpha\cos\beta \\ -\sin\alpha\sin\beta & -\cos\beta & \cos\alpha\sin\beta \\ \cos\alpha & 0 & \sin\alpha \end{bmatrix}$$
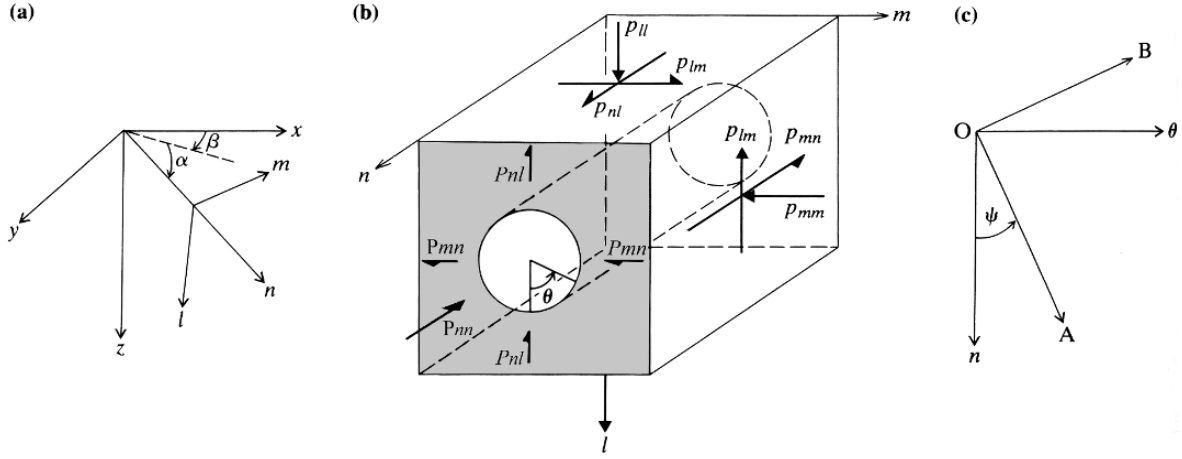
In Figure 5.5b, the location of a point on the wall of the borehole is defined by the angle θ measured clockwise in the l, m plane. Boundary stresses at the point

(b)
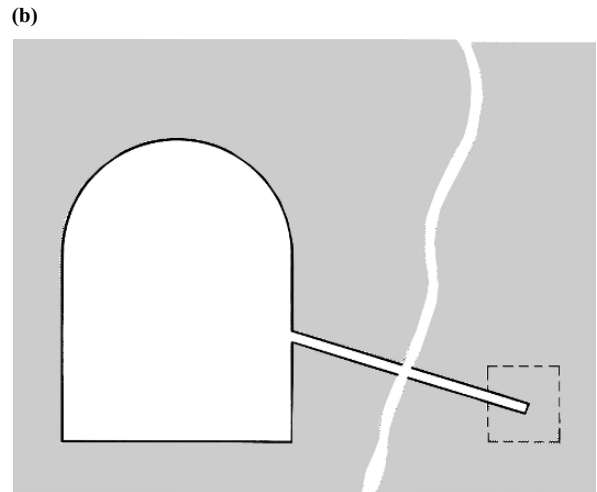
Figure 5.4 (a) A triaxial strain cell (of CSIRO design), and (b), (c), (d) its method of application.

(c)

strain cell

(d)
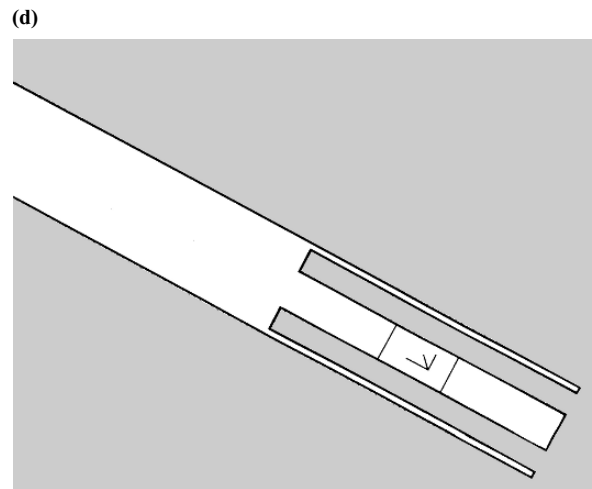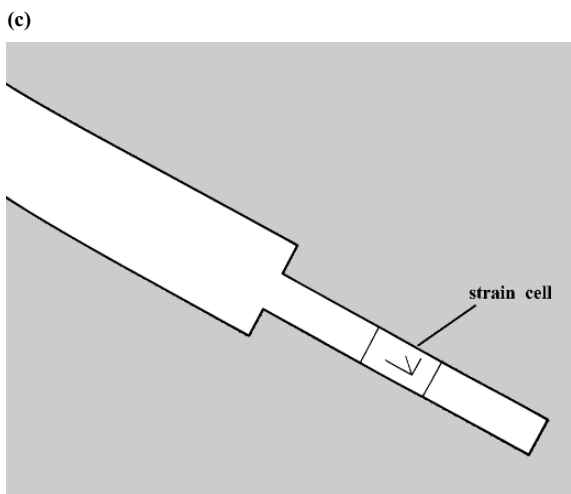
Figure 5.5 (a) Definition of hole local axes; (b) field stress components relative to hole local axes and position co-ordinate angle, θ; (c) reference axes on hole wall.

are related to the local field stresses, for an isotropic elastic medium, by the expressions

$$\sigma_{rr} = \sigma_{r\theta} = \sigma_{rn} = 0$$

$$\sigma_{\theta\theta} = p_{ll}(1 - 2\cos 2\theta) + p_{mm}(1 + 2\cos 2\theta) - 4p_{lm}\sin 2\theta$$

$$\sigma_{nn} = p_{nn} + 2\nu(-p_{ll}\cos 2\theta + p_{mm}\cos 2\theta - 2p_{lm}\sin 2\theta) \qquad (5.3)$$

$$\sigma_{\theta n} = 2p_{mn}\cos \theta - 2p_{nl}\sin \theta$$

Equations 5.3 define the non-zero boundary stress components, $\sigma_{\theta\theta}, \sigma_{\theta n}, \sigma_{nn}$, relative to the n, θ axes, aligned respectively with the hole axis, and the orthogonal direction which is tangential, in the l, m plane, to the hole boundary. Another set of right Cartesian axes, OA, OB, may be embedded in the hole boundary, as shown in Figure 5.5c, where the angle Ψ defines the rotation angle from the n, θ axes to the OA, OB axes. The normal components of the boundary stress, in the directions OA, OB are given by

$$\sigma_A = \tfrac{1}{2}(\sigma_{nn} + \sigma_{\theta\theta}) + \tfrac{1}{2}(\sigma_{nn} - \sigma_{\theta\theta})\cos 2\Psi + \sigma_{\theta n}\sin 2\Psi$$

$$\sigma_B = \tfrac{1}{2}(\sigma_{nn} + \sigma_{\theta\theta}) - \tfrac{1}{2}(\sigma_{nn} - \sigma_{\theta\theta})\cos 2\Psi - \sigma_{\theta n}\sin 2\Psi \qquad (5.4)$$

Suppose the direction OA in Figure 5.5c coincides with the orientation and location of a strain gauge used to measure the state of strain in the hole wall. Since plane stress conditions operate at the hole boundary during the stress relief process, the measured normal strain component is related to the local boundary stress components by

$$\varepsilon_A = \frac{1}{E}(\sigma_A - \nu\sigma_B)$$

or

$$E\varepsilon_A = \sigma_A - \nu\sigma_B \qquad (5.5)$$

Substituting the expressions for σ_A, σ_B (equations 5.4) in equation 5.5, and then substituting equations 5.3 in the resulting expression, gives the required relation

150

between the local state of strain in the hole wall and the field stresses as

$$
\begin{aligned}
E\varepsilon_A = {} & p_{ll}\{\tfrac{1}{2}[(1-\nu)-(1+\nu)\cos 2\Psi] - (1-\nu^2)(1-\cos 2\Psi)\cos 2\theta\} \\
& + p_{mm}\{\tfrac{1}{2}[(1-\nu)-(1+\nu)\cos 2\Psi] + (1-\nu^2)(1-\cos 2\Psi)\cos 2\theta\} \\
& + p_{nn}\tfrac{1}{2}[(1-\nu)+(1+\nu)\cos 2\Psi] \\
& - p_{lm}2(1-\nu^2)(1-\cos 2\Psi)\sin 2\theta \\
& + P_{mn}2(1+\nu)\sin 2\Psi \cos\theta \\
& - p_{nl}2(1+\nu)\sin 2\Psi \sin\theta
\end{aligned}
\tag{5.6a}
$$

or

$$
a_1 p_{ll} + a_2 p_{mm} + a_3 p_{nn} + a_4 p_{lm} + a_5 p_{mn} + a_6 p_{nl} = b
\tag{5.6b}
$$

Equations 5.6a and 5.6b indicate that the state of strain in the wall of a borehole, at a defined position and in a particular orientation, specified by the angles θ and Ψ, is determined linearly by the field stress components. In equation 5.6b, the coefficients $a_i(i=1-6)$ can be calculated directly from the position and orientation angles for the measurement location and Poisson's ratio for the rock. Thus if six independent observations are made of the state of strain in six positions/orientations on the hole wall, six independent simultaneous equations may be established. These may be written in the form

$$
[\mathbf{A}][\mathbf{p}] = [\mathbf{b}]
\tag{5.7}
$$

where $[\mathbf{p}]$ represents a column vector formed from the stress components $p_{ll}, p_{mm}, p_{nn}, p_{lm}, p_{mn}, p_{nl}$. Provided the positions/orientations of the strain observations are selected to ensure a well conditioned coefficient matrix $[\mathbf{A}]$, equation 5.7 can be solved directly for the field stress components p_{ll}, p_{lm}, etc.. A Gaussian elimination routine, similar to that given by Fenner (1974), presents a satisfactory method of solving the set of equations.

The practical design of a triaxial strain cell usually provides more than the minimum number of six independent strain observations. The redundant observations may be used to obtain large numbers of equally valid solutions for the field stress tensor (Brady *et al.*, 1976). These may be used to determine a locally averaged solution for the ambient state of stress in the zone of influence of the stress determination. Confidence limits for the various parameters defining the field stress tensor may also be attached to the measured state of stress.

5.3.3 Flatjack measurements

Stress measurement using strain gauge devices is usually performed in small-diameter holes, such that the volume of rock whose state of stress is sampled is about $10^{-3}\,\mathrm{m}^3$. Larger volumes of rock can be examined if a larger diameter opening is used as the measurement site. For openings allowing human access, it may be more convenient to measure directly the state of stress in the excavation wall, rather than the state of strain. This eliminates the need to determine or estimate a deformation modulus for the rock mass. The flatjack method presents a particularly attractive procedure for determination of the boundary stresses in an opening, as it is a null method, i.e. the

151

(a)

(b)
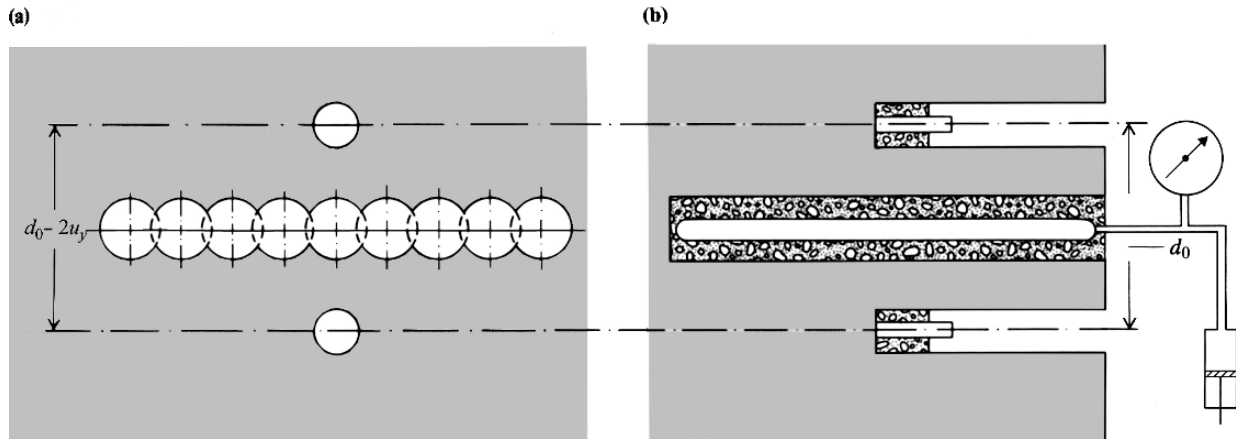
Figure 5.6 (a) Core drilling a slot for a flatjack test and (b) slot pressurisation procedure.

measurement system seeks to restore the original, post-excavation local state of stress at the experiment site. Such methods are intrinsically more accurate than those relying on positive disturbance of the initial condition whose state is to be determined.

Three prerequisites must be satisfied for a successful *in situ* stress determination using flatjacks. These are:

(a) a relatively undisturbed surface of the opening constituting the test site;
(b) an opening geometry for which closed-form solutions exist, relating the far-field stresses and the boundary stresses; and
(c) a rock mass which behaves elastically, in that displacements are recoverable when the stress increments inducing them are reversed.

The first and third requirements virtually eliminate the use as a test site of an excavation developed by conventional drilling and blasting. Cracking associated with blasting, and other transient effects, may cause extensive disturbance of the elastic stress distribution in the rock and may give rise to non-elastic displacements in the rock during the measurement process. The second requirement restricts suitable opening geometry to simple shapes. An opening with circular cross section is by far the most convenient.

The practical use of a flatjack is illustrated in Figure 5.6. The jack consists of a pair of parallel plates, about 300 mm square, welded along the edges. A tubular non-return connection is provided to a hydraulic pump. A measurement site is established by installing measurement pins, suitable for use with a DEMEC or similar deformation gauge, in a rock surface and perpendicular to the axis of the proposed measurement slot. The distance d_0 between the pins is measured, and the slot is cut, using, for example, a series of overlapping core-drilled holes. Closure occurs between the displacement measuring stations. The flatjack is grouted in the slot, and the jack pressurised to restore the original distance d_0 between the displacement monitoring pins. The displacement cancellation pressure corresponds closely to the normal stress component directed perpendicular to the slot axis prior to slot cutting.

Determination of the field stresses from boundary stresses using flatjacks follows a procedure similar to that using strain observations. Suppose a flatjack is used to measure the normal stress component in the direction OA in Figure 5.5c, i.e. the plane of the flatjack slot is perpendicular to the axis OA. If σ_A is the jack cancellation

152

pressure, substitution of the expressions for $\sigma_{\theta\theta}$, σ_{nn}, $\sigma_{\theta n}$ (equations 5.3) into the expression for σ_A(equation 5.4) yields

$$
\begin{aligned}
\sigma_A = {} & p_{ll}\tfrac{1}{2}\{(1 - \cos 2\Psi) - 2\cos 2\theta[(1 + \nu) - (1 - \nu)\cos 2\Psi]\} \\
& + p_{mm}\tfrac{1}{2}\{(1 - \cos 2\Psi) + 2\cos 2\theta[(1 + \nu) - (1 - \nu)\cos 2\Psi]\} \\
& + p_{nn}\tfrac{1}{2}(1 + \cos 2\Psi) - p_{lm}\,2\sin 2\theta\{(1 + \nu) - (1 - \nu)\cos 2\Psi\} \\
& + p_{mn}\,2\sin 2\Psi\cos\theta - p_{nl}\,2\sin 2\Psi\sin\theta
\end{aligned}
\tag{5.8}
$$

or

$$
C_1 p_u + C_2 p_{mm} + C_3 p_{nn} + C_4 p_{lm} + C_5 p_{mn} + C_6 p_{nl} = \sigma_A
\tag{5.9}
$$

Equation 5.9 confirms that the state of stress in any position/orientation in the hole boundary is linearly related to the field stress components, by a set of coefficients which are simply determined from the geometry of the measurement system. Thus if six independent observations of σ_A are made at various locations defined by angles θ and Ψ, a set of six simultaneous equations is established:

$$
[\mathbf{C}][\mathbf{p}] = [\sigma]
\tag{5.10}
$$

The terms of the coefficient matrix $[\mathbf{C}]$ in this equation are determined from θ and Ψ for each boundary stress observation, using equation 5.8.

In the design of a measurement programme, the boundary stress measurement positions and orientations must be selected carefully, to ensure that equations 5.10 are both linearly independent and well conditioned. The criterion for a poorly conditioned set of equations is that the determinant of the $[\mathbf{C}]$ matrix is numerically small compared with any individual term in the matrix.

5.3.4 Hydraulic fracturing

A shortcoming of the methods of stress measurement described previously is that close access to the measurement site is required for operating personnel. For example, hole depths of about 10 m or less are required for effective use of most triaxial strain cells. Virtually the only method which permits remote determination of the state of stress is the hydraulic fracturing technique, by which stress measurements can be conducted in deep boreholes such as exploration holes drilled from the surface.

The principles of the technique are illustrated in Figure 5.7. A section of a borehole is isolated between inflatable packers, and the section is pressurised with water, as shown in Figure 5.7a. When the pressure is increased, the state of stress around the borehole boundary due to the field stresses is modified by superposition of hydraulically-induced stresses. If the field principal stresses in the plane perpendicular to the hole axis are not equal, application of sufficient pressure induces tensile circumferential stress over limited sectors of the boundary. When the tensile stress exceeds the rock material tensile strength, fractures initiate and propagate perpendicular to the hole boundary and parallel to the major principal stress, as indicated in Figure 5.7b. Simultaneously, the fluid pressure falls in the test section. After relaxation of the pressure and its subsequent re-application, the peak borehole pressure achieved is less than the initial boundary fracturing pressure by an amount corresponding to the tensile strength of the rock material.

153
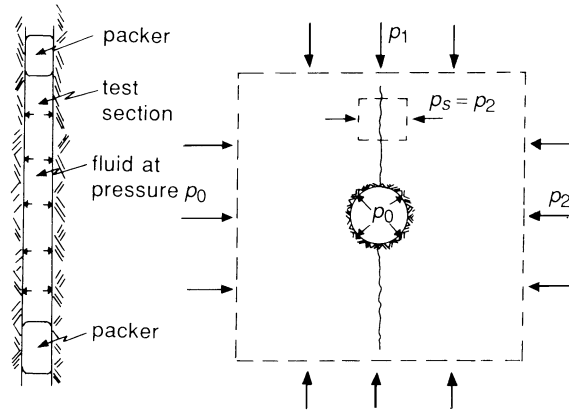
Figure 5.7 Principles of stress measurement by hydraulic fracturing: (a) packed-off test section; (b) cross section of hole, and fracture orientation relative to plane principal stresses.

A record of borehole pressure during an hydraulic fracturing experiment, in which typically several cycles of pressure application and decline are examined, is shown in Figure 5.8. Two key parameters defined on the borehole pressure record are the instantaneous shut-in pressure p_s and the crack re-opening pressure p_r. The shut-in pressure or fracture closure pressure defines the field principal stress component perpendicular to the plane of the fracture. As suggested by Figure 5.7b, this corresponds to the minor principal stress p_2 acting in the plane of section. The crack re-opening pressure is the borehole pressure sufficient to separate the fracture surfaces under the state of stress existing at the hole boundary. The crack re-opening pressure, the shut-in pressure and the pore pressure, u, at the test horizon may be used to estimate the major principal stress in the following way.

The minimum boundary stress, σ_{min}, around a circular hole in rock subject to biaxial stress, with field stresses of magnitudes p_1 and p_2, is given by

$$\sigma_{min} = 3p_2 - p_1 \tag{5.11}$$

When a pressure p_0 is applied to the interior of the borehole, the induced tangential stress $\sigma_{\theta\theta}$ at the hole wall is

$$\sigma_{\theta\theta} = -p_0$$
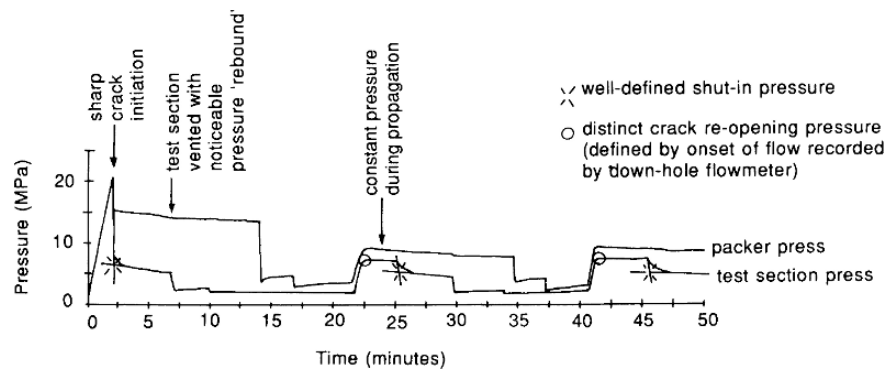
Figure 5.8 Pressure vs. time record for a hydraulic fracturing experiment (after Enever and Chopra, 1986).

154

The minimum tangential boundary stress is obtained by superimposing this stress on that given by equation 5.11, i.e.

$$\sigma_{\min} = 3p_2 - p_1 - p_0 \tag{5.12}$$

and the minimum effective boundary stress is

$$\sigma'_{\min} = 3p_2 - p_1 - p_0 - u \tag{5.13}$$

The crack re-opening pressure p_r corresponds to the state of borehole pressure p_0 where the minimum effective boundary stress is zero, i.e. introducing p_r in equation 5.13

$$3p_2 - p_1 - p_r - u = 0$$

or

$$p_1 = 3p_2 - p_r - u \tag{5.14}$$

Because $p_2 = p_s$, equation 5.14 confirms that the magnitudes of the major and minor plane principal stresses p_1 and p_2 can be determined from measurements of shut-in pressure p_s and crack re-opening pressure p_r. The orientation of the principal stress axes may be deduced from the position of the boundary fractures, obtained using a device such as an impression packer. The azimuth of the major principal stress axis is defined by the hole diameter joining the trace of fractures on opposing boundaries of the hole.

Although hydraulic fracturing is a simple and apparently attractive stress measurement technique, it is worth recalling the assumptions implicit in the method. First, it is assumed that the rock mass is continuous and elastic, at least in the zone of influence of the hole and the hydraulically induced fractures. Second, the hole axis is assumed to be parallel to a field principal stress axis. Third, the induced fracture plane is assumed to include the hole axis. If any of these assumptions is not satisfied, an invalid solution to the field stresses will be obtained. A further limitation is that it provides only plane principal stresses, and no information on the other components of the triaxial stress field. The usual assumption is that the vertical normal stress component is a principal stress, and that it is equal to the depth stress.

5.3.5 *Other methods of estimating the* in situ *state of stress*

Compared with overcoring, flatjacks and hydraulic fracturing, some other methods of estimating the *in situ* state of stress are attractive by virtue of the relative ease with which the raw data for the stress determination can be recovered. Of particular interest in this regard are methods based on borehole breakouts, stress history gauging through the Kaiser effect, and differential strain curve analysis or deformation rate analysis.

The borehole breakout method described by Zoback *et al.* (1985) relies on the state of stress around a borehole being sufficient to cause compressive fracture at preferred locations around the hole boundary. Assuming a principal stress direction is parallel to the borehole axis and that the principal stress field in the plane perpendicular to the hole axis is anisotropic, the Kirsch equations and a knowledge of the rock material

155

strength properties allow an estimate of the state of stress immediately outside the zone of influence of the borehole. Widely used in the petroleum industry for estimating the state of stress in deep reservoirs, the method is reviewed in detail by Zoback *et al.* (2003). An example of its application in hard rock is provided by Paillet and Kim (1987).

Development and application of a method for *in situ* stress measurement based on the Kaiser effect is described by Villaescusa *et al.* (2002). The Kaiser effect is an expression of the immediately preceding maximum stress to which a specimen of rock has been subjected, and provides a method of estimating the recent stress history of a core sample recovered from a borehole. For a specimen containing microcracks, such as brittle rock, uniaxial loading is aseismic until a stress threshold is reached characteristic of the earlier stress magnitude it experienced. Application of the Kaiser effect in estimating the complete stress tensor relies on a capacity to determine reliably the magnitudes of the preceding normal stresses applied to the specimen in various directions. This is done by monitoring the emission of acoustic pulses during loading of small undercores recovered from the larger, oriented drill core taken from the ground. By Kaiser-effect gauging of preceding stresses in six undercores in six mutually independent orientations, it is possible to invert the normal stresses to recover the field stresses which the large core experienced *in situ*. The advantage of the method is the relative convenience and ease of application and the related low cost.

Anelastic strain recovery (Voight, 1968) exploits the relaxation which a rock core experiences after it is isolated from the stressed host rock mass. The time-dependent strains are measured with strain gauges, the principal strains calculated, and the total strains are estimated by assuming direct proportionality between total strains and the anelastic strains.

Differential strain curve analysis (Roegiers, 1989) or deformation rate analysis (Villaescusa *et al.*, 2002) are similar in principle to Kaiser effect gauging of the recent stress history of a sample of rock. When a core is taken from the ground, relaxation of normal stress allows microcracks to open. In axial loading of undercores taken from a larger core, closure of open microcracks is indicated by a clear change in the slope of the axial stress-normal strain plot. The related value of the applied normal stress is taken to correspond to the normal stress existing in the ground immediately prior to recovery of the core. If closure stresses are determined for undercores taken in six mutually independent orientations, then as for Kaiser-effect gauging, it is possible to invert the stress data to recover the field principal stresses and their orientations.

### 5.4 Presentation of *in situ* stress measurement results

The product of a stress measurement exercise is the set of six components of the field stress tensor, usually expressed relative to a set of local axes for the measurement hole. These yield the stress components expressed relative to the global axes by a simple transformation. The principal stress magnitudes and orientations are then determined from these quantities using the methods described in Chapter 2. If a single determination is made of the field stress tensor, the orientations of the principal stress axes can be plotted directly on to a stereonet overlay as shown in Figure 5.9. The value of this procedure is that the required mutual orthogonality of the principal

$\sigma_1 : \sigma_2 : \sigma_3 = 1.0 : 0.6 : 0.4$
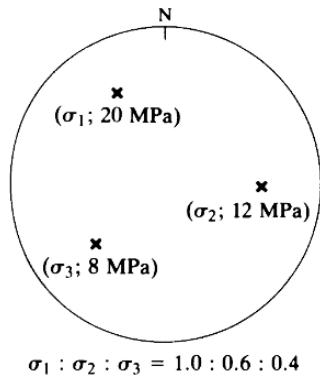
Figure 5.9 Presentation of principal stress data on lower hemisphere stereographic projection.

stress directions can be determined by direct measurement. It therefore provides a useful check on the validity and consistency of the solution for the principal stresses. Other points of confirmation of the correctness of the solution are readily established by considering the magnitudes of the various stress invariants, calculated from the several sets of components (expressed relative to different sets of reference axes) of the field stress tensor.

In the case where redundant experimental observations have been collected, many independent solutions are possible for the *in situ* stress tensor. The methods suggested by Friday and Alexander (Brady *et al.*, 1976) can then be used to establish mean values of the components and principal directions of the stress tensor. An example of the way in which an over-determination of experimental parameters can be used is illustrated in Figure 5.10. More than 1000 independent solutions for the field stresses allowed construction of histograms of principal stress magnitudes, and contour plots of principal stress directions. Presumably, greater reliability can be attached to the mean values of principal stress magnitudes and orientations obtained from these plots, than to any single solution for the field stresses. The usual tests for consistency can be applied to the mean solution in the manner described earlier.
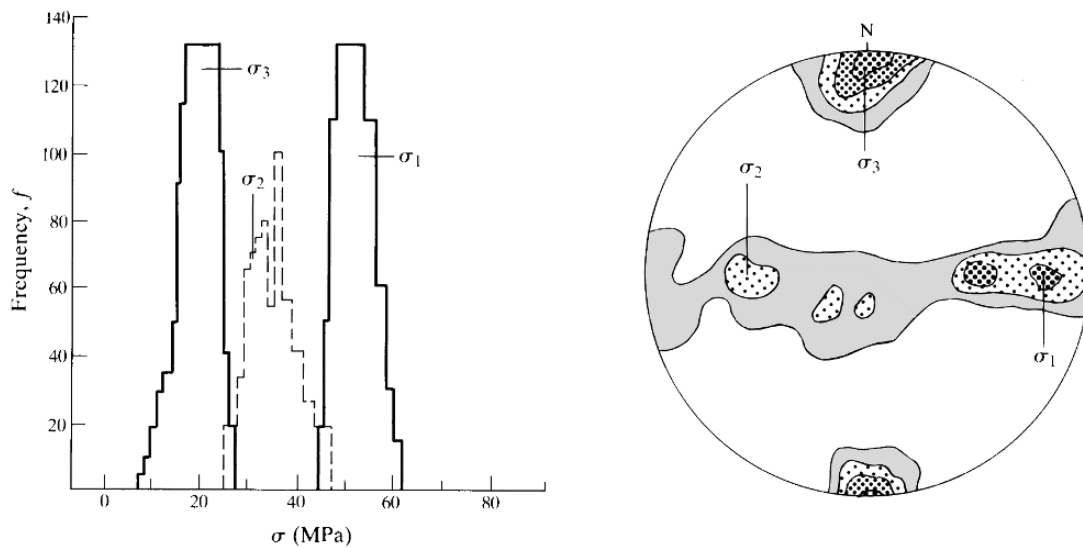
Figure 5.10 Histogram plots of principal stress frequencies and contour plots and principal stress orientations obtained from redundant strain observations.

A number of other assessments, in addition to those to test the internal consistency of a solution for the field stresses, can be performed to take account of specific site conditions. A primary requirement is that the ambient state of stress cannot violate the *in situ* failure criterion for the rock mass. As was noted in Chapter 4, establishing a suitable rock mass failure criterion is not a simple procedure process, but an essential proposition is that the field stresses should not violate the failure criterion for the intact rock material. The latter rock property may be established from standard laboratory tests on small specimens. Since the *in situ* strength of rock is typically much less than the strength measured on small specimens, the proposed test may not be a sensitive discriminant of the acceptability of a field stress determination. However, it ensures that widely inaccurate results are identified and re-examined.

157

A second determinant of the mechanical acceptability of an *in situ* stress measurement is derived from the requirement for conditions of static equilibrium on pervasive planes of weakness in the rock mass. Application of this criterion is best illustrated by example. Suppose a fault plane has the orientation 295°/50° (dip direction/dip), and that the measured *in situ* stress field is defined by:

$$\sigma_1, \text{ magnitude 15 MPa, dips 35° towards 085°;}$$
$$\sigma_2, \text{ magnitude 10 MPa, dips 43° towards 217°;}$$
$$\sigma_3, \text{ magnitude 8 MPa, dips 27° towards 335°.}$$

The groundwater pressure at the measurement horizon is 2.8 MPa, and the angle of friction for the fault surface 25°. These data can be used to determine the normal and resultant shear stress components acting on the fault, and thus to calculate the angle of friction on the fault surface required to maintain equilibrium.

The given data are applied in the following way. When plotted on a stereonet, the direction angles (α, β, γ) between the principal axes and the pole to the fault plane are measured directly from the stereonet as (24°, 71°, 104°). These yield direction cosines (l_1, l_2, l_3) of (0.914, 0.326, −0.242) of the fault normal relative to the principal stress axes. The effective principal stresses are given by

$$\sigma_1' = 12.2 \text{ MPa}$$
$$\sigma_2' = 7.2 \text{ MPa}$$
$$\sigma_3' = 5.2 \text{ MPa}$$

Working now in terms of effective stresses, the resultant stress is given by

$$R = \left(l_1^2\, \sigma_1'^2 + l_2^2\, \sigma_2'^2 + l_3^2\, \sigma_3'^2\right)^{1/2} = 11.46 \text{ MPa}$$

and the normal stress by

$$\sigma_n' = l_1^2\, \sigma_1' + l_2^2\, \sigma_2' + l_3^2\, \sigma_3' = 11.26 \text{ MPa}$$

The resultant shear stress is

$$\tau = \left(R^2 - \sigma_n'^2\right)^{1/2} = 2.08 \text{ MPa}$$
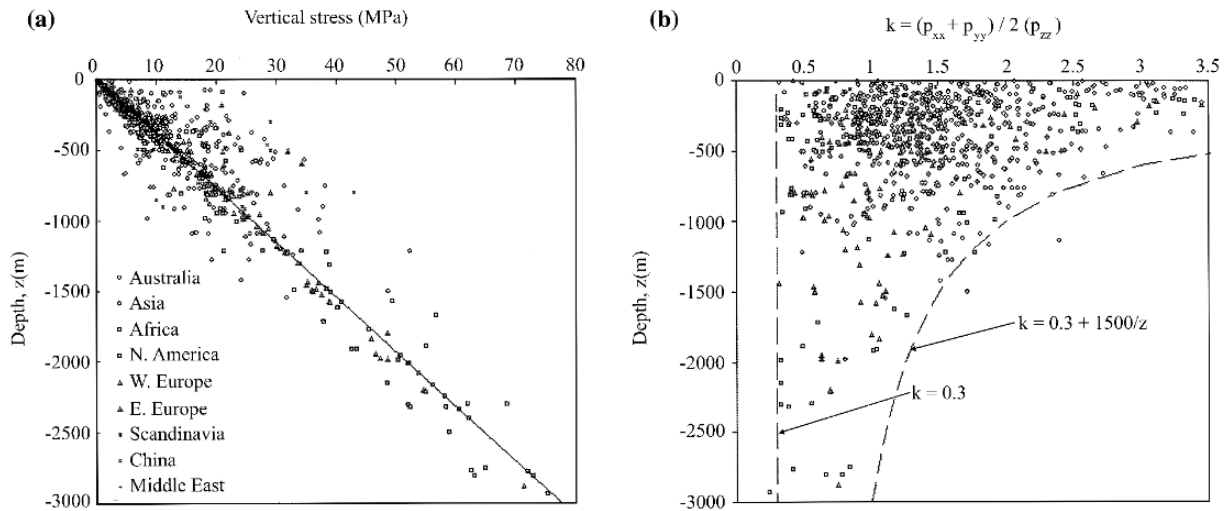
The angle of friction mobilised by the given state of stress on the plane is

$$\phi_{\text{mob}} = \tan^{-1}(2.08/11.26) = 10.5°$$

Since ϕ_{mob} is less than the measured angle of friction for the fault, it is concluded that the *in situ* state of stress is compatible with the orientation and strength properties of the fault. It is to be noted also that a similar conclusion could be reached by some simple constructions on the stereonet. Clearly, the same procedures would be followed for any major structural feature transgressing the rock mass.

For the example considered, the measured state of stress was consistent with static equilibrium on the plane of weakness. In cases where the field stresses apparently violate the equilibrium condition, it is necessary to consider carefully all data related to

(a) Vertical stress (MPa)

(b) $k = (p_{xx} + p_{yy}) / 2 (p_{zz})$

Legend for (a):
- Australia
- Asia
- Africa
- N. America
- W. Europe
- E. Europe
- Scandinavia
- China
- Middle East

In (b): $k = 0.3 + 1500/z$; $k = 0.3$

Figure 5.11 Variation with depth below surface of (a) measured values of *in situ* vertical stress, p_{zz}, and (b) ratio of average measured horizontal stresses to the vertical stress (data compiled by Windsor, 2003, after Aydan and Kawamoto, 1997).

the problem. These include such factors as the possibility of a true cohesive component of discontinuity strength and the possible dilatant properties of the discontinuity in shear. Questions to be considered concerning stress measurement results include the probable error in the determination of both principal stress magnitudes and directions, and the proximity of the stress measurement site to the discontinuity. Thus the closer the measurement site to the discontinuity, the more significance to be attached to the no-slip criterion. Only when these sorts of issues have been considered in detail should the inadmissibility of a solution for the field stress tensor be decided.

5.5 Results of *in situ* stress measurements

A comprehensive collation of the results of measurement of the pre-mining state of stress, at the locations of various mining, civil and petroleum engineering projects, reported by Brown and Hoek (1978), was updated by Windsor (2003). The results presented in Figure 5.11 consist of data for about 900 determinations of *in situ* states of stress. Although data exist for depths extending to 7 km, those presented are for depths down to 3 km, which is the range of interest in most mining projects. The first observation from this figure is that the measurements of p_{zz} (in MPa) are scattered about the trend line

$$p_{zz} = 0.027z$$

where z (in m) is the depth below ground surface. Since 27 kN m^{-3} represents a reasonable average unit weight for most rocks, it appears that the vertical component of stress is closely related to depth stress. A further observation concerns the variation with depth of the parameter k, defined as the ratio of the average of the horizontal stresses to the vertical stresses: i.e.

$$k = (p_{xx} + p_{yy})/2p_{zz}$$

The data are bounded on the lower side by $k = 0.3$, while the upper bound is defined

159

by the expression

$$k = 0.3 + 1500/z$$

where z is the depth below the ground surface in metres.

At shallow depth, values of k vary widely and are frequently much greater than unity. At increasing depth, the variability of the ratio decreases and the upper bound tends towards unity. Some of the variability in the stress ratio at shallow depths and low stress levels may be due to experimental error. However, the convergence of the ratio to a value of unity at depth is consistent with the principle of time-dependent elimination of shear stress in rock masses. The postulate of regression to a lithostatic state by viscoplastic flow is commonly referred to as Heim's Rule (Talobre, 1957).

The final observation arising from inspection of Figures 5.11a and b is a confirmation of the assertion made at the beginning of this chapter. The virgin state of stress in a rock mass is not amenable to calculation by any known method, but must be determined experimentally. In jointed and fractured rock masses, a highly variable stress distribution is to be expected, and indeed has been confirmed by several investigations of the state of stress in such settings. For example, Bock (1986) described the effect of horizontal jointing on the state in a granite, confirming that each extensive joint defined a boundary of a distinct stress domain. In the analysis of results from a jointed block test, Brown *et al.* (1986) found that large variations in state of stress occurred in the different domains of the block generated by the joints transgressing it. Richardson *et al.* (1986) reported a high degree of spatial variation of the stress tensor in foliated gneiss, related to rock fabric, and proposed methods of deriving a representative solution of the field stress tensor from the individual point observations. In some investigations in Swedish bedrock granite, Carlsson and Christiansson (1986) observed that the local state of stress is clearly related to the locally dominant geological structure.

These observations of the influence of rock structure on rock stress suggest that a satisfactory determination of a representative solution of the *in situ* state of stress is probably not possible with a small number of random stress measurements. The solution is to develop a site-specific strategy to sample the stress tensor at a number of points in the mass, taking account of the rock structure. It may then be necessary to average the results obtained, in a way consistent with the distribution of measurements, to obtain a site representative value.

The natural state of stress near the earth's surface is of world-wide interest, from the points of view of both industrial application and fundamental understanding of the geomechanics of the lithosphere. For example, industrially the topic is of interest in mining and petroleum engineering and hazardous waste isolation. On a larger scale, the topic is of interest in tectonophysics, crustal geomechanics and earthquake seismology. From observations of the natural state of stress in many separate domains of the lithosphere, 'world stress maps' have been assembled to show the relation between the principal stress directions and the megascopic structure of the earth's crust. An example is shown in Figure 5.12, due to Reinecker *et al.* (2003). The map is a section of the world map showing measurements of horizontal principal stresses in and around the Australasian plate.

The value of such a map in mining rock mechanics is that it presents some high level information on orientations of the horizontal components of the pre-mining

160
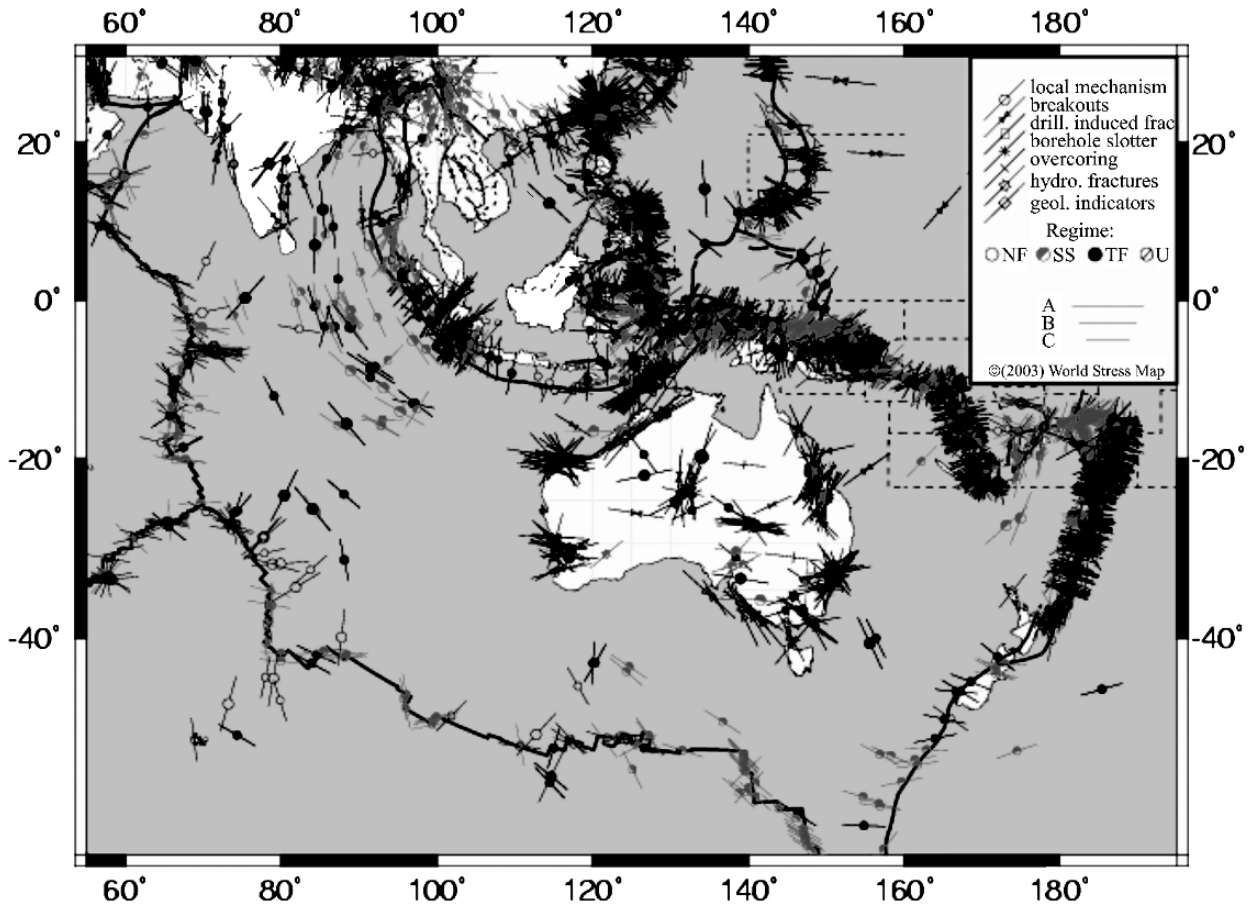
Figure 5.12 A section of the stress map of the world, showing orientations of horizontal principal stresses in and around the Australasian plate (after Reinecker *et al.*, 2003).

principal stresses which can be incorporated in site investigations and preliminary design and scoping studies. A map of this type is also valuable in other fields of resource engineering. For example, considering the Australian continental land mass, Mukhamadiev *et al.* (2001) showed that, by analysis of the horizontal principal stress orientations, after constructing the principal stress trajectories it was possible to deduce the macroscopic state of stress throughout the continental block. An important result from the analysis was that it suggested the existence of a singular point in the interior of the Australian continent, where the ratio k of the horizontal stresses is unity. This has significant implications for exploitation of petroleum and geothermal energy resources in the region, which might depend on hydraulic fracture treatments for their economic recovery.

Problems

1 At a particular site, the surface topography can be represented in a vertical cross section by a vertical cliff separating horizontal, planar ground surfaces, as shown in the figure (a) below. The upper and lower surfaces AB and CD can be taken to

extend infinite distances horizontally from the toe of the 100 m high cliff. The effect of the ground above the elevation D′CD can be treated as a wide surcharge load on a half-space.

(a) The stress components due to a line load of magnitude P on a half space are given by

$$\sigma_{rr} = \frac{2P \sin \theta}{\pi r}$$

$$\sigma_{\theta\theta} = \sigma_{r\theta} = 0$$

where r and θ are defined in figure (b).

Relative to x, z reference axes, show that the stress components due to the strip load defined in figure (c) are given by

$$\sigma_{xx} = \frac{p}{2\pi}[2(\theta_2 - \theta_1) + (\sin 2\theta_2 - \sin 2\theta_1)]$$

$$\sigma_{zz} = \frac{p}{2\pi}[2(\theta_2 - \theta_1) - (\sin 2\theta_2 - \sin 2\theta_1)]$$

$$\sigma_{zx} = \frac{p}{2\pi}[\cos 2\theta_1 - \cos 2\theta_2]$$

(b) If the unit weight of the rock is 27 kN m^{-3}, calculate the stress components induced at a point P, 80 m vertically below the toe of the cliff, by the surcharge load.

(c) If the state of stress at a point Q remote from the toe of the cliff and on the same elevation as P, is given by $\sigma_{xx} = 2.16$ MPa, $\sigma_{zz} = 3.24$ MPa, $\sigma_{zx} = 0$, estimate the magnitudes and orientations of the plane principal stresses at P.


(a)   (b)   (c)
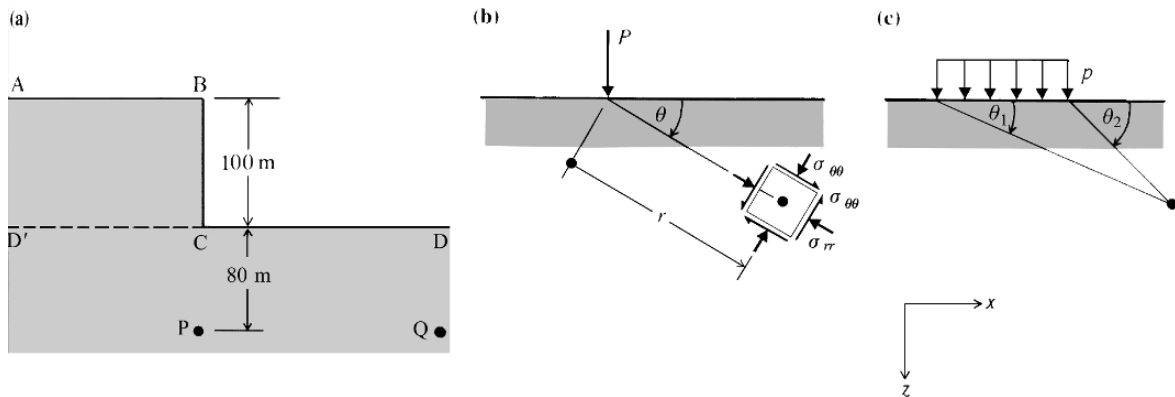
2 An element of rock 800 m below ground surface is transgressed by a set of parallel, smooth continuous joints, dipping as shown in the figure below. The fissures are water filled below an elevation 100 m below the ground surface. The vertical stress component p_{zz} is a principal stress, and equal to the depth stress. From the calculated depth stress, p_{zz}, calculate the range of possible magnitudes of the horizontal stress component, p_{xx}. The unit weight of the rock mass is 26 kN m^{-3}, and the unit weight

of water 9.8 kN m^{-3}. The resistance to slip on the joints is purely frictional, with an angle of friction ϕ' of 20°.

State any assumptions used in deriving the solution.
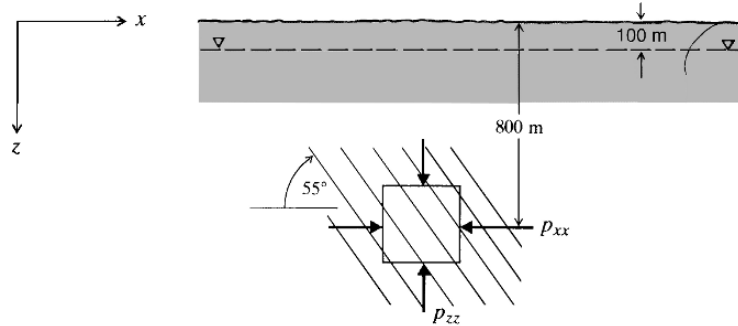
3 In an underground mine, flatjacks were used to measure the state of stress in the walls and crown of a long horizontal tunnel of circular cross section. Independent observations indicated that the long axis of the tunnel was parallel to a field principal stress. For slots cut parallel to the tunnel axis, the cancellation pressures were 45 MPa in both side walls, at the midheight of the tunnel, and 25 MPa in the crown. For slots cut in each side wall, perpendicular to the tunnel axis and at the tunnel midheight, the cancellation pressures were 14.5 MPa.

(a) By considering the symmetry properties of equations 5.3 defining boundary stresses around a circular hole in a triaxial stress field, deduce the principal stress directions.
(b) Calculate the magnitudes of the field principal stresses, assuming $\nu = 0.25$.

4 A CSIRO hollow inclusion strain cell was used in an overcoring experiment to determine the state of strain in the walls of a borehole. The borehole was oriented 300°/70°. Using the angular co-ordinates and orientations defined in Figure 5.5, the measured states of strain (expressed in microstrains) in the wall of the hole were, for various θ and Ψ:

θ° \ Ψ°	0°	45°	90°	135°
0°	—	213.67	934.41	821.11
120°	96.36	—	349.15	131.45
240°	96.36	—	560.76	116.15

Young's modulus of the rock was 40 GPa, and Poisson's ratio, 0.25.

(a) Set up the set of nine equations relating measured strain and gauge location. (Note that, for $\Psi = 0°$, identical equations are obtained, independent of θ.)
(b) Select the best conditioned set of six equations, and solve for the field stresses, expressed relative to the hole local axes.
(c) Transform the field stresses determined in (b) to the mine global axes (x – north, y – east, z – down).

163

(d) Determine the magnitudes of the field principal stresses, and their orientations relative to the mine global axes.
(Note: This problem is most conveniently handled with a calculator capable of solving six simultaneous equations.)

5 Measurement of the state of stress in a rock mass produced the following results:

$$\sigma_1, \text{ of magnitude 25 MPa, is oriented } 109°/40°;$$

$$\sigma_2, \text{ of magnitude 18 MPa, is oriented } 221°/25°;$$

$$\sigma_3, \text{ of magnitude 12 MPa, is oriented } 334°/40°.$$

The groundwater pressure at the measurement site is 8 MPa. A fault, oriented $190°/60°$, is cohesionless, and has an estimated angle of friction of $\phi' = 20°$.

Comment on the consistency of this set of observations, and describe any other subsequent investigations you might consider necessary.